Available online at www.sciencedirect.com
SCIENCE DIRECT
International Journal of Heat and Mass Transfer 49 (2006) 1813–1819
International Journal of HEAT and MASS TRANSFER
www.elsevier.com/locate/ijhmt

Local heat transfer during reflux condensation mode in a U-tube with and without noncondensible gases

Kyung-Won Lee [a,*], Hee Cheon NO [a], In-Cheol Chu [b], Young Min Moon [a], Moon-Hyun Chun [a]

[a] *Department of Nuclear and Quantum Engineering, Korea Advanced Institute of Science and Technology, 373-1 Guseong-dong, Yuseong-gu, Daejeon 305-701, Republic of Korea*

[b] *Department of Thermal-Hydraulics Safety Research, Korea Atomic Energy Research Institute, P.O. Box 105, Yuseong-gu, Daejeon 305-600, Republic of Korea*

Received 30 November 2004
Available online 19 January 2006

Abstract

A series of experiments was performed to investigate the local heat transfer phenomenon inside a U-tube in a reflux condensation mode. A total of 477 data (108 for pure steam flow conditions and 369 for steam–air flow conditions) for the local heat transfer coefficients were obtained for various inlet flow rates of steam and air under atmospheric conditions. Based on the steam–air experimental results, a new correlation applicable to the reflux condensation mode is developed using the degradation factor. The new correlation includes the effects of the flow rates of the condensate and the noncondensible gases (air) on the heat transfer coefficient. Most of our data agree with the predicted values with a RMS error of 27.4%.

Keywords: Reflux condensation; Local heat transfer coefficient; Noncondensible gases; Degradation factor

1. Introduction

Reflux condensation cooling operation is one of alternative operation modes when a residual heat removal system is lost during a mid-loop operation or a small-break loss of coolant accident in a pressurized water reactor. It is important in core cooling. During the reflux condensation cooling operation, three distinctive modes may occur in the U-tubes of a steam generator (SG) depending on the operating conditions. First, in a filmwise reflux condensation mode, the vertical countercurrent flow of steam and condensate is formed in the upflow side of the SG U-tubes. Second, in the oscillatory (or total reflux condensation) mode, the reactor primary coolant may be decreased when the riser section of the U-tubes is blocked by a single-phase liquid column formed above the two-phase region. Third, in the natural circulation (or carry-over) mode, the liquid column can be carried over to the other side of the U-tube, and the steam flows concurrently with its condensate [1].

When analyzing the safety analysis of nuclear power plants during the reflux condensation, it is very important to determine the mechanism that governs heat transfer phenomenon in SG U-tubes. As a result, the thermal-hydraulic phenomena in U-tubes during reflux condensation have been extensively studied, experimentally and theoretically. In the 1980s, for example, such studies were undertaken by Chen et al. [2], Chun and Park [3], and Chen et al. [4]. More recently, studies in this field have been reported by Pilon et al. [5], Chou and Chen [6], Moon et al. [7], Thumm et al. [8], and Vierow et al. [9]. Several larger scale experiments have also been carried out with the aid of integral test facilities such as BETHSY [10] and IIST [11,12].

Although numerous studies have been conducted on the reflux condensation in scaled-down and full-scale facilities, there is a paucity of experimental data to show the local

* Corresponding author. Tel.: +82 42 869 3857; fax: +82 42 869 3810.
E-mail address: leekw@nsys.kaist.ac.kr (K.-W. Lee).

0017-9310/$ - see front matter © 2005 Elsevier Ltd. All rights reserved.
doi:10.1016/j.ijheatmasstransfer.2005.11.011

Nomenclature

D	tube diameter [m]
d	thermocouple diameter [mm]
g	gravitational acceleration [m/s^2]
h, HTC	heat transfer coefficient [W/m^2 K]
ID	tube inner diameter [mm]
i	enthalpy [J/kg]
Ja	Jacob number
k	thermal conductivity [W/m K]
$\dot{m}$	mass flow rate [kg/s]
P	pressure [MPa]
q	heat transfer rate [W]
q''	heat flux [W/m^2]
r	tube radius [m]
Re	Reynolds number
RMS error	root mean square error, $\sqrt{\frac{1}{N}\sum\left(\frac{h_{cal}-h_{exp}}{h_{cal}}\right)^2}$
T	temperature [°C]
T/C	thermocouple
W_{air}	air mass fraction

Greek symbols

δ	condensate film thickness [m]
μ	viscosity [Ns/m^2]
ρ	density [kg/m^3]
σ	uncertainty
Γ	condensate mass flow rate per unit width [kg/s m]

Subscripts

cw	secondary side cooling water
exp	experimental value
f	liquid (water) phase
g	gas phase, steam–air mixture
i	tube inner side
n	central location between adjacent thermocouples
s	steam
STS	stainless steel (or SUS)
w	tube wall
1	inner T/C location
2	outer T/C location
x	axial location of thermocouple
Δx	axial distance between thermocouples [m]

heat transfer phenomena in the presence of noncondensible gases during the filmwise reflux condensation mode.

Moon et al. and Vierow et al. measured the local heat transfer coefficients (HTCs) for the reflux condensation. They used a single vertical tube surrounded by a concentric coolant jacket in which flow regime was forced convection. However, during the mid-loop operation, the heat transfer condition at the secondary side of SG U-tubes is a natural convection or pool boiling. As a result, the use of the coolant jacket may affect the heat transfer phenomena.

The main purpose of this study is to evaluate the local condensation heat transfer with and without noncondensible gases. In addition, the present study aims at quantifying the effects of SG secondary side pool temperature and the flow rates of steam and noncondensible gases (air) on the heat transfer phenomenon.

2. Experiments

2.1. Experimental apparatus

Fig. 1 shows a schematic diagram of the experimental apparatus. The main components of the system are the test section, the steam and air supply system, the sensors and devices that measure the temperature and flow rates, and the data acquisition system.

To simulate the geometry of the SG U-tubes in a Korea standard nuclear power plant (KSNP, Ulchin 3 and 4 units, ID of the U-tubes = 0.01692 m), we installed a U-tube with the inner diameter of 0.0162 m in a rectangular pool (314.4 mm × 117.2 mm × 3600 mm). The U-tube was made of stainless steel (SUS 304). The height and thickness of the U-tube are 2.8 m and 0.0055 m, respectively.

The U-tube is fully equipped with 32 T-type thermocouples to evaluate the local HTCs. Fig. 2 shows the locations of thermocouples. The local heat fluxes are measured at 12 different elevations along the U-tube. We directly measure the temperature gradient of the U-tube wall to evaluate the local heat flux through a U-tube wall, and then determine the local HTCs.

Steam, which is supplied by a 200 kW electric steam boiler, passes through two steam–water separators, a flow control needle valve, and an accurately calibrated turbine flow meter before it finally flows into the test section. The two steam–water separators are used to supply the test section with a sufficiently dry saturated steam or slightly superheated steam. Furthermore, a preheater is used to maintain the air temperature at a constant level equal to the steam temperature. The flow rate of air is controlled by a needle valve and measured with a rotameter.

2.2. Test parameters and test procedure

The controllable test parameters are the pool temperature of the SG secondary side and the inlet flow rates of steam and air. A series of experiments has been conducted for various combinations of the test parameters under atmospheric pressure conditions summarized in Table 1.

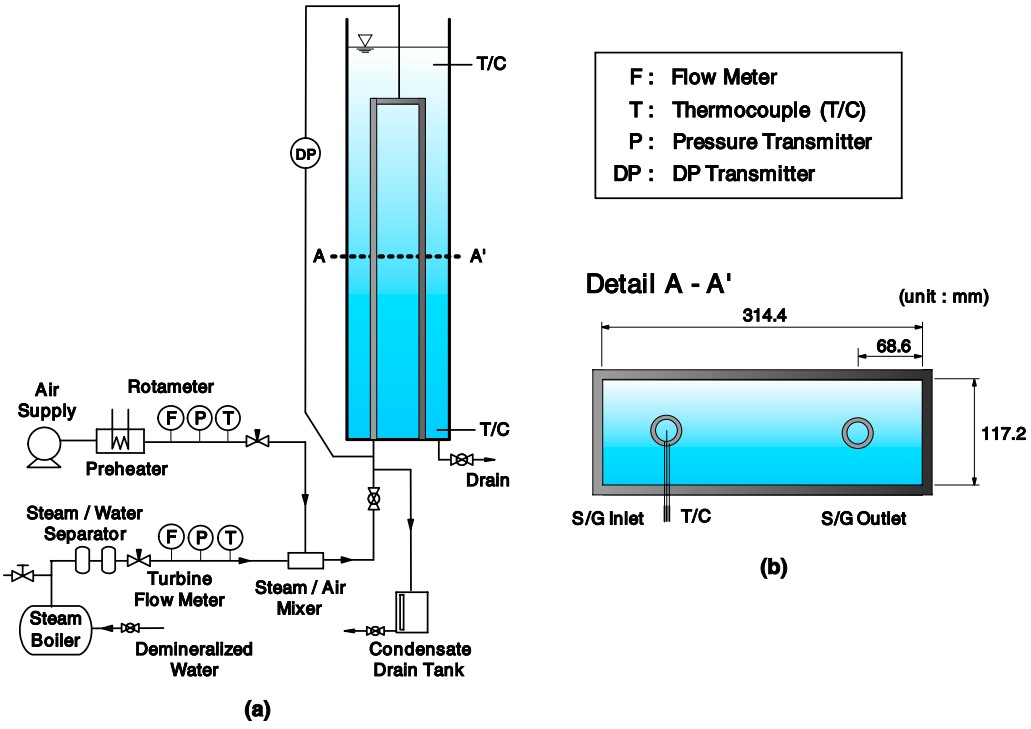

Fig. 1. Schematic diagram of the experimental apparatus: (a) test loop with U-tube, (b) cross-section of test section.

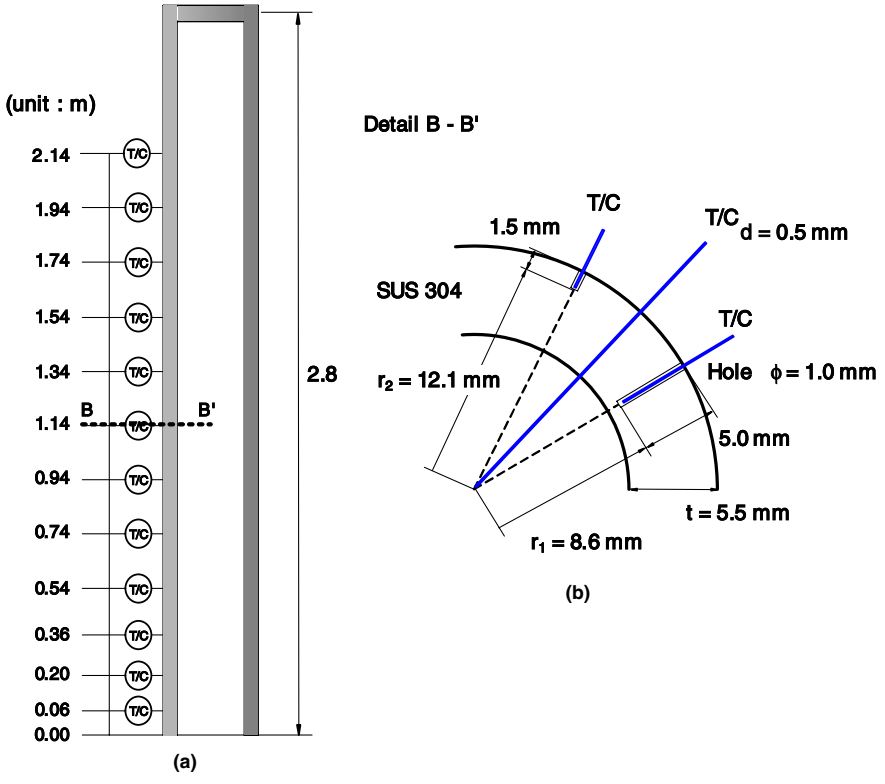

Fig. 2. Locations of thermocouples: (a) T/C locations, (b) cross-section of U-tube.

The Reynolds number (Re) ranges about 16–273 for the condensate and 375–6285 for the steam (131–5922 for the steam–air mixture). The air mass fraction (W_{air}) and the Jacob number (Ja) range 0.02–0.83 and 0.014–0.1, respectively. Table 1 also shows Moon et al.'s experimental ranges.

Table 1
Experimental conditions

Experiments	Present work		Moon et al. [7]
	Pure steam	Steam–air	Steam–air
P (MPa)	0.1	0.1	0.1, 0.15, 0.25
$\dot{m}_{s,in}$ (kg/h)	1.08–3.59	1.08–3.59	1.38–3.28
$\dot{m}_{air,in}$ (kg/h)	–	0.057–0.57	0.28–2.44
$\dot{m}_{cw}$ (kg/h)	–	–	90–226.8
T_{cw} (°C)	40–75	25–40	6–28
Re_f	16–273	3–246	1.5–176.3
Re_s	375–6285	91–6179	108.6–4803.1
Re_g	–	131–5922	794–4755.6
W_{air}	–	0.02–0.83	0.12–0.96
Ja	–	0.014–0.1	0.03–0.123
No. of data	108	369	165

The experimental procedure for a given test is as follows: (1) after allowing a sufficient time to reach a quasi-steady state, we set the inlet flow rates of steam and air to the desired values. (2) When the test condition reaches a steady state, we measure all the local temperatures of U-tube wall. (3) We repeat this procedure for each test.

To prevent the steam from condensing prematurely before it flows into the test section, we allow sufficient heating time (about 1 h) before starting to acquire data.

3. Data reduction and analysis

Fig. 3 shows the control volume that describes the heat transfer process during the reflux condensation. For local condensation, the HTC at any axial location x from the U-tube inlet can be expressed as

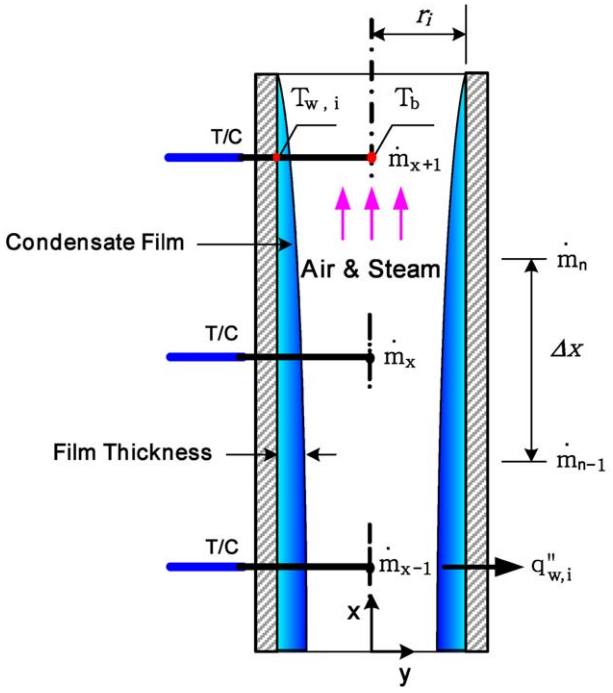

Fig. 3. Control volume for reflux condensation.

$$h(x) = \frac{q''_{w,i}(x)}{T_b(x) - T_{w,i}(x)}. \quad (1)$$

Thus, the local condensation HTC, $h(x)$ is deduced from the measured heat flux ($q''_{w,i}$), the temperature at the tube center (T_b), and the temperature at the tube inner wall ($T_{w,i}$) at any x.

The temperature at the tube center can be measured directly. The heat flux through the tube wall at any axial position (x) can be calculated from the temperature gradient in the U-tube wall by a steady-state heat conduction equation for a cylindrical geometry, Eq. (2):

$$q''_{w,i}(x) = k_{STS}(x)\frac{T_1(x) - T_2(x)}{r_i \ln(r_2/r_1)}. \quad (2)$$

The temperature at the tube inner wall can be deduced from the heat flux as given by Eq. (3):

$$T_{w,i}(x) = T_1(x) + q''_{w,i}(x)\frac{r_i \ln(r_1/r_i)}{k_{STS}(x)} = T_1(x) + \frac{\ln(r_1/r_i)}{\ln(r_2/r_1)}[T_1(x) - T_2(x)], \quad (3)$$

where the subscripts 1 and 2 denote the radial positions at which the thermocouples were installed in the U-tube as shown in Fig. 2(b). The thermal conductivity of tube wall, $k_{STS}(x)$, was calculated based on the average temperature of T_1 and T_2.

For a complete reflux condensation, all the injected steam is completely condensed in the upflow side of S/G U-tubes and the conservation of mass at the steady state yields Eq. (4):

$$\dot{m}_s(x) = \dot{m}_f(x). \quad (4)$$

The local mass flow rate of the condensate (or steam) can be calculated by following equations:

$$\dot{m}_n = \dot{m}_{n-1} - \frac{q_{\Delta x}}{i'_{fg}}, \quad (5)$$

$$\dot{m}_x = \frac{\dot{m}_{n-1} + \dot{m}_n}{2}, \quad (6)$$

where $q_{\Delta x}$ is the heat transfer rate from the primary side to the secondary side of the S/G U-tube between distance Δx; and i'_{fg} is the modified latent heat of vaporization given by

$$i'_{fg} = i_{fg} + 0.68C_{p,f}(T_b - T_{w,i}). \quad (7)$$

The modified latent heat of vaporization includes the effects of the condensate subcooling and the nonlinear temperature distribution through the condensate film due to energy convection.

The definitions of the dimensionless parameters used in the present study are as follows:

$$Re_f = \frac{4\Gamma}{\mu_f} = \frac{4\dot{m}_f}{\pi D_i \mu_f}, \qquad Re_s = \frac{4\dot{m}_s}{\pi D_i \mu_s},$$
$$Re_g = \frac{4\dot{m}_g}{\pi D_i \mu_g}, \qquad Ja = \frac{C_{p,f}(T_b - T_{w,i})}{i_{fg}}, \quad (8)$$
$$W_{air} = \frac{\dot{m}_{air}}{\dot{m}_{air} + \dot{m}_s}.$$

In using these equations, we evaluate all liquid properties at the film temperature, $T_f = (T_b + T_{w,i})/2$, and we evaluate i_{fg} at the saturation temperature, T_{sat}. The viscosity of steam–air mixture, μ_g, can be calculated by Wilke's method [13].

4. Results and discussion

4.1. Temperature distributions along the tube

The temperature distributions along the upflow side of the S/G U-tube, with and without noncondensible gases, are shown in Fig. 4. For all experiments, the temperature difference between the top and the bottom of the secondary side pool of the S/G is less than 2 °C.

For a pure steam flow, all the injected steam is completely condensed within 1.8 m from the tube inlet for the present experimental range, and there are clear temperature changes between the active condensation zone (where the condensation occurs) and the passive condensation zone (where no condensation occurs). For the steam–air flow, however, the condensation length is relatively long and the temperature distribution along the tube axial direction tends to decrease gradually due to the effect of noncondensible gases. The condensation length increases when the pool temperature of the S/G secondary side or the flow rates of steam and air increase.

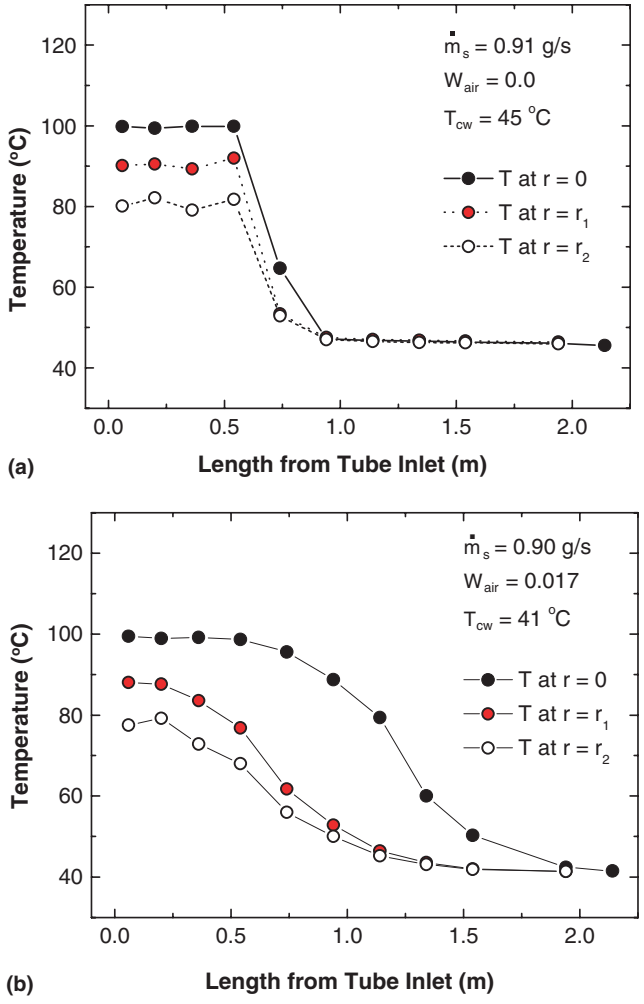

Fig. 4. Temperature profiles along the tube: (a) without noncondensible gases, (b) with noncondensible gases.

4.2. Parametric effects of the flow rates of steam and air on HTCs

For the present operating conditions, the ranges of the local heat flux ($q''_{w,i}$) measured at the tube inner wall are 17,947–75,570 W/m^2 for a pure steam flow and 4429–67,227 W/m^2 for a steam–air flow. The ranges of the local HTCs are founded to be around 4940–27,313 W/m^2 K (most of the HTCs are less than 15,000 W/m^2 K) for the pure steam flow and 109–6940 W/m^2 K for the steam–air flow experiments.

Fig. 5 shows the effects of the flow rates of steam and air on the HTCs. As expected, the local HTCs increase as the steam flow rate increases, whereas they decrease as the air mass fraction increases. The local HTCs decrease markedly by a very small amount of air mass fraction (about 2%).

In all our experimental results for the steam–air flow, the maximum HTC is observed at the tube inlet. However, in some experiments conducted by Moon et al. and Vierow et al., the maximum HTC was observed a little downstream (about 10–25 cm) from the tube inlet. To evaluate the local heat fluxes, we measure directly the temperature gradient at the tube wall, whereas Moon et al. and Vierow et al. measured the temperature profile of coolant along the tube to evaluate the local heat fluxes. Therefore, the reason for the difference in the HTC profiles may be due to the entrance effect of coolant jackets.

4.3. Development of empirical correlation

In Fig. 6, the present experimental data for the pure steam flow are plotted in the form of HTCs versus the

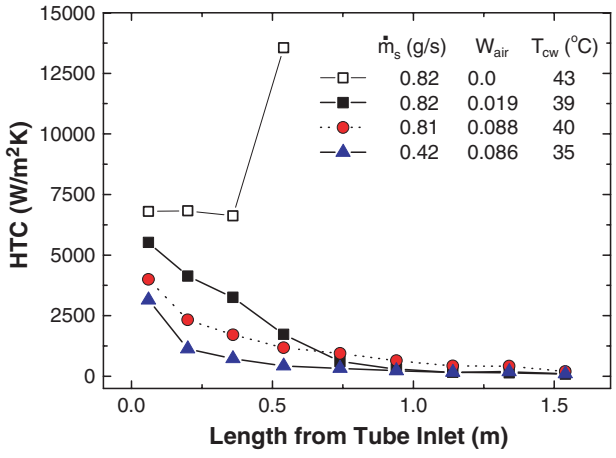

Fig. 5. Effects of the steam flow rate and noncondensible gases on the HTCs.

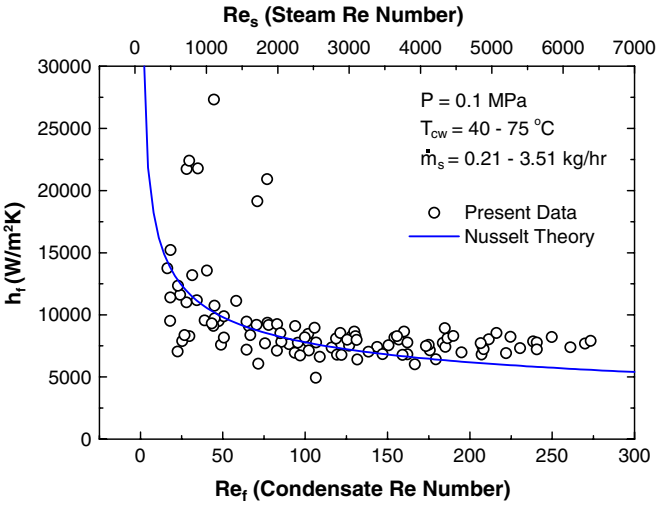

Fig. 6. Comparison of experimental data with the Nusselt theory in the absence of noncondensible gases.

condensate Reynolds number (and the steam Reynolds number), and they are compared with the predictions of the Nusselt theory [14]. The results show, regardless of the steam flow rate and the pool temperature, most of the local condensation HTCs are nearly constant (approximately 7500 W/m^2 K) along the tube axial direction except at low condensate Reynolds number ($Re_f < 75$) where the condensate thickness is very thin. Although the present experimental conditions differ from those assumed in the Nusselt theory, the data for the pure steam flow generally agree with the predictions of the Nusselt theory. However, for relatively high steam Reynolds numbers (that is, larger than 3500), the present data are slightly higher than the results predicted by the theory, mainly due to the interfacial waves [4,8].

In the case of pure steam condensation, the condensate film acts as the only resistance to the heat transfer. However, when noncondensible gases are present, the main resistance to the heat transfer is the liquid–steam interface where the noncondensible gases carried by the steam accumulate. To quantify the parametric effect of the flow rates of steam and noncondensible gases (air) on the HTC, we develop a new correlation, on the basis of the degradation factor, that can be applied to the reflux condensation mode.

The degradation factor, F, which shows the ratio of decrease in the heat transfer capability in the presence of noncondensible gases, is defined as the ratio of the local experimental condensation HTC (h_{exp}) to the local value by the Nusselt theory (h_f). The value of h_f is defined by Eq. (9), and the thickness of the condensate film, δ, is calculated from Eq. (10) as follows:

$$h_f = \frac{k_f}{\delta}, \tag{9}$$

$$\delta = \left[\frac{3\mu_f^2 Re_f}{4\rho_f(\rho_f - \rho_g)g}\right]^{1/3}. \tag{10}$$

In developing the new correlation, we use Moon et al.'s experimental data and our own steam–air experimental data. The experiment of Moon et al. was conducted with a single vertical tube (with an ID of 16.56 mm and a length of 2.4 m) surrounded by a concentric coolant jacket (with an ID of 57.2 mm). Their steam flow rate is comparable to ours but the inlet air mass fractions in their experiments (11.8–55%) are higher than ours (1–24%). The definitions of dimensionless parameters are the same in both experiments, and therefore a direct comparison between the two is possible. To evaluate the local heat flux through the U-tube wall, we use the temperature gradient in the tube wall, whereas Moon et al. used the net increase in the coolant temperature of the secondary side.

The degradation factor, F, is principally a function of the condensate Reynolds number (Re_f), the steam Reynolds number (Re_s), the steam–air mixture Reynolds number (Re_g), the air mass fraction (W_{air}) and the Jacob number (Ja).

The root mean square (RMS) error of the correlation with Re_f was smaller than that of the correlation with Re_s or Re_g. Therefore, by using multiple linear regression analysis, we develop the following correlation with three parameters of Re_f, W_{air}, and Ja:

$$F = \frac{h_{exp}}{h_f} = 4.88 \times 10^{-4} Re_f^{0.59} W_{air}^{-0.29} Ja^{-0.89}. \tag{11}$$

The applicable ranges of Eq. (11) are

$1.5 < Re_f < 246$,

$0.02 < W_{air} < 0.96$,

and

$0.014 < Ja < 0.123$.

Fig. 7 shows the comparison of the measured HTCs with the HTCs derived from Eq. (11). With some exceptions, most of our data agree with the predicted values

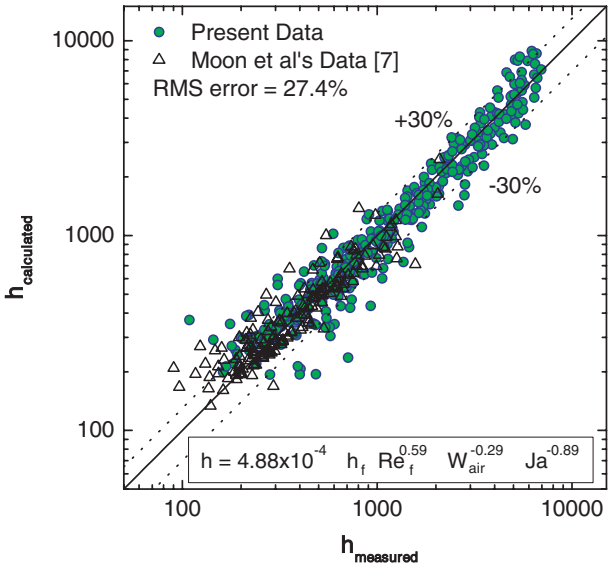

Fig. 7. Comparison of measured HTCs with predicted HTCs.

Table 2
Estimated uncertainties of major parameters

	Parameters	Bias limit	Precision limit
Independent parameters	Temperature T_1, T_2, T_b (°C)	0.8	0.5
	T/C position error (m)	0.0003	–
Dependent parameters	Inner wall temperature (°C)	0.81–1.68	0.5
	Thermal conductivity $k_{STS}(x)$ (W/m K)	0.0147	0.0092
	Local HTCs (%)	2.2–20.6	0.9–6.6
Uncertainty of local heat transfer coefficients σ_h (%)		2.4–21.7 (average 7.2%)	

within ±30% (with a RMS error of 27.4%). The HTCs in the experiment of Moon et al. are lower than the HTCs in our experimental data because of the relatively high inlet air mass fractions.

4.4. Uncertainty analysis

To examine the error in the values of the measured heat flux, we compare the enthalpy inflow (the inlet mass flow rate of the steam multiplied by steam enthalpy) and the heat flux integrated over the U-tube height (condensation length). The error of the height-averaged heat flux is in the range of −10.2% to 3.8%.

To analyze the uncertainties of the local HTCs, we used the error propagation method [15], and we compute the total uncertainty of the local HTCs (σ_h) with the aid of the root-sum-square method of the bias limit (σ_B) and the precision limit (σ_P). The estimated uncertainties of the HTCs are in the range of 2.4–21.7% (at an average of 7.2%) and these uncertainties mainly resulted from the measurement error of the thermocouples. The uncertainties of the HTCs by the error of thermocouple positions are in the range of 0.3–15.2% (at an average of 3.8%). Table 2 summarizes these results.

5. Conclusions

With a series of experiments, we investigated the local HTCs during reflux condensation mode in a U-tube. From our results, we make the following conclusions:

(1) For the pure steam flow, most of the local condensation HTCs are nearly constant (approximately 7500 W/m^2 K) along the tube axial direction except at low condensate Reynolds number ($Re_f < 75$), regardless of the steam flow rate and the pool temperature. However, when noncondensible gases (air) are present, the local condensation HTCs increase as the steam flow rate increases but decrease as the air mass fraction increases.

(2) Our experimental results obtained for pure steam flows generally agree with the predictions of the Nusselt theory. However, at relatively high steam Reynolds number (that is, larger than 3500), our results are slightly higher than the predictions of the Nusselt theory, mainly due to the interfacial waves.

(3) To include the effect of flow rates of steam and noncondensible gases on HTCs, we develop, on the basis of the degradation factor, a new correlation that can be applied to the reflux condensation mode. We correlate the degradation factor in terms of the condensate Reynolds number, the air mass fraction, and the Jacob number as given by Eq. (11). Most of our data agree with the predicted values with a RMS error of 27.4%.

References

[1] Q. Nguyen, S. Banerjee, Analysis of experimental data on condensation in an inverted U-tube, EPRI/NP-4091, 1985.
[2] S.J. Chen, J.G. Reed, C.L. Tien, Reflux condensation in a two-phase closed thermosyphon, Int. J. Heat Mass Transfer 27 (9) (1984) 1587–1594.
[3] M.H. Chun, J.W. Park, Reflux condensation phenomena in vertical U-tubes with and without noncondensible gases, ASME Paper 84-WA/HT-2, 1984.
[4] S.L. Chen, F.M. Gerner, C.L. Tien, General film condensation correlations, Exp. Heat Transfer 1 (1987) 93–107.
[5] L. Pilon, G. Geffraye, T. Chataing, Validation of the CATHARE film condensation model on COTURNE experiment, in: The 6th International Conference on Nuclear Engineering (ICONE-6), ICONE-6379, San Diego, CA, 1998.
[6] G.-H. Chou, J.-C. Chen, A general modeling for heat transfer during reflux condensation inside vertical tubes surrounded by isothermal fluid, Int. J. Heat Mass Transfer 42 (1999) 2299–2311.
[7] Y.M. Moon, H.C. NO, H.S. Park, Y.S. Bang, Assessment of RELAP5/MOD3.2 for reflux condensation experiment, NUREG/IA-0181, 2000.
[8] S. Thumm, Ch. Philipp, U. Gross, Film condensation of water in a vertical tube with countercurrent vapor flow, Int. J. Heat Mass Transfer 44 (2001) 4245–4256.
[9] K. Vierow, T. Nagae, T. Wu, Experimental investigation of reflux condensation heat transfer in PWR steam generator tubes in the presence of noncondensible gases, in: The 10th International Topical Meeting on Nuclear Reactor Thermal Hydraulics (NURETH-10), Seoul, Korea, 2003.
[10] D. Dumont, G. Lavialle, B. Noel, R. Deruaz, Loss of residual heat removal during mid-loop operation: BETHSY experiments, Nucl. Eng. Des. 149 (1994) 365–374.
[11] C.H. Lee, T.J. Liu, Y.S. Way, D.Y. Hsia, Investigation of mid-loop operation with loss of PHR at INER integral system test (IIST) facility, Nucl. Eng. Des. 163 (1996) 349–358.
[12] T.J. Liu, Reflux condensation behavior in a U-tube steam generator with or without noncondensables, Nucl. Eng. Des. 204 (2001) 221–232.
[13] C.R. Wilke, A viscosity equation for gas mixtures, J. Chem. Phys. 18 (4) (1950) 517–519.
[14] W. Nusselt, Die Oberflachenkondensation des Wasserdampfes dsca, Z. Vereines Deutsch Ing. 60 (1916) 541–546, 569–575.
[15] S.J. Kline, F.A. McClintock, Describing uncertainties in single-sample experiments, Mech. Eng. 75 (1953) 3–8.